Supplement information for the manuscript

Synthesis, Structure, and Polymorphic Transitions of Praseodymium(III) and Neodymium(III) Borohydride, $Pr(BH_4)_3$ and $Nd(BH_4)_3$

SeyedHosein Payandeh GharibDoust[a]*, Michael Heere[b,c], Carlo Nervi[d], Magnus H. Sørby[b], Bjørn C. Hauback[b], Torben R. Jensen[a]*

[a]Center for Materials Crystallography, Interdisciplinary Nanoscience Center (iNANO) and Department of Chemistry, Aarhus University, Langelandsgade 140, DK-8000 Århus C, Denmark
[b]Department for Neutron Materials Characterization, Institute for Energy Technology, NO-2027 Kjeller, Norway.
[c]Research Neutron Source Munich (FRM2) and Karlsruhe Institute of Technology (KIT), Institute for Applied Materials—Energy Storage Systems (IAM-ESS), 76344 Eggenstein, Germany
[d]Department of Chemistry, NIS and CIRCC, University of Turin, Via P. Giuria 9, I-10125 Torino, Italy

Keywords: borohydride, rare earth, hydrogen storage, decomposition, halide free

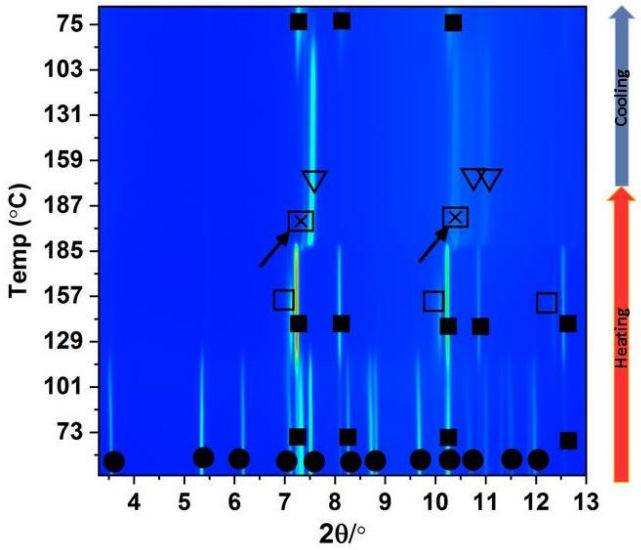

Figure S1 *In-situ* SR-XRPD data of $Pr(^{11}BD_4)_3S(CH_3)_2$ (**s1**) compound under p(Ar) = 1 bar. $\Delta T/\Delta t$ = 5 °C/min (λ = 0.7129 Å). Symbols: ● $Pr(^{11}BD_4)_3S(CH_3)_2$; ■ α-$Pr(^{11}BD_4)_3$ $Pa\bar{3}$; □ β-$Pr(^{11}BD_4)_3$ $Fm\bar{3}c$; ⊠ β''-$Pr(^{11}BD_4)_3$ $Fm\bar{3}c$ and ▽ for r-$Pr(^{11}BD_4)_3$ $R\bar{3}c$.

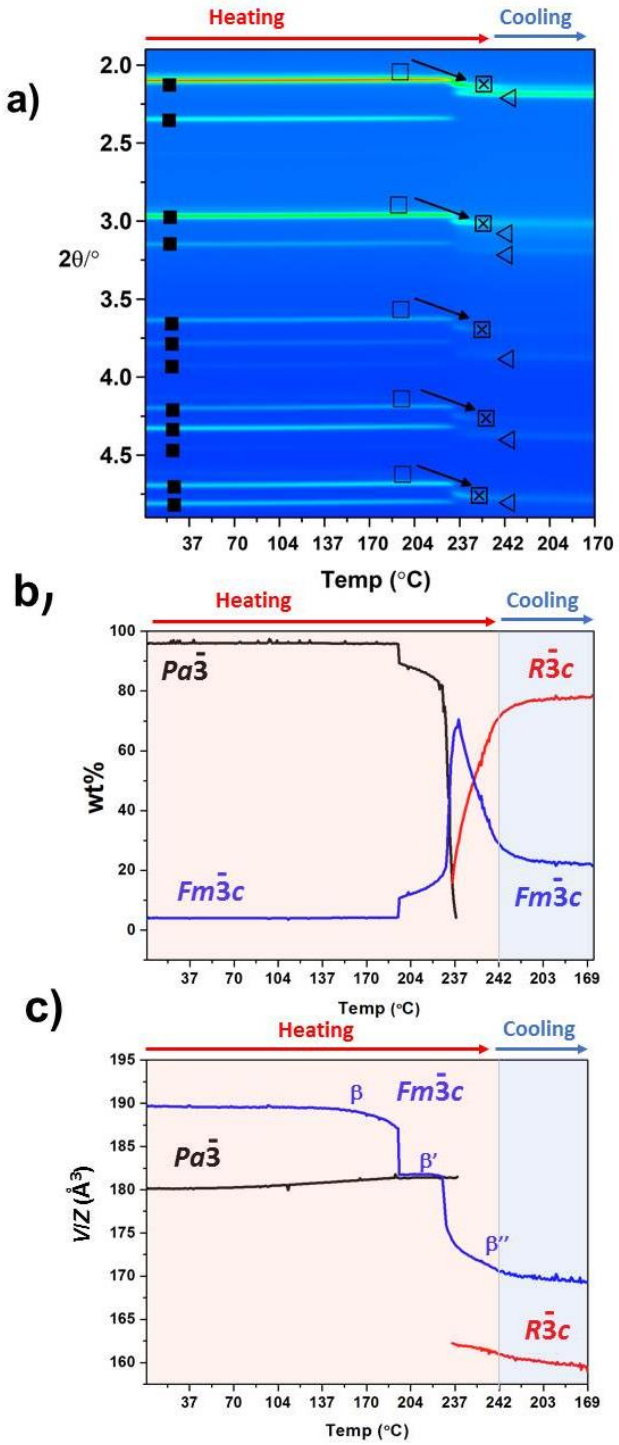

Figure S2 a) *In-situ* SR-XRPD data of $Pr(BH_4)_3$ (**s3**) under *p*(Ar) = 1 bar. $\Delta T/\Delta t$ = 5 °C/min (λ = 0.2072 Å). b) Sample composition and c) *V*/*Z* of each phase extracted by Rietveld refinement of SR-XRPD data, symbols: ■ for α-$Pr(BH_4)_3$ ($Pa\bar{3}$); □ for β-$Pr(BH_4)_3$ ($Fm\bar{3}c$); ☒ for β''-$Pr(BH_4)_3$ ($Fm\bar{3}c$) and ◁ for r-$Pr(BH_4)_3$ ($R\bar{3}c$).

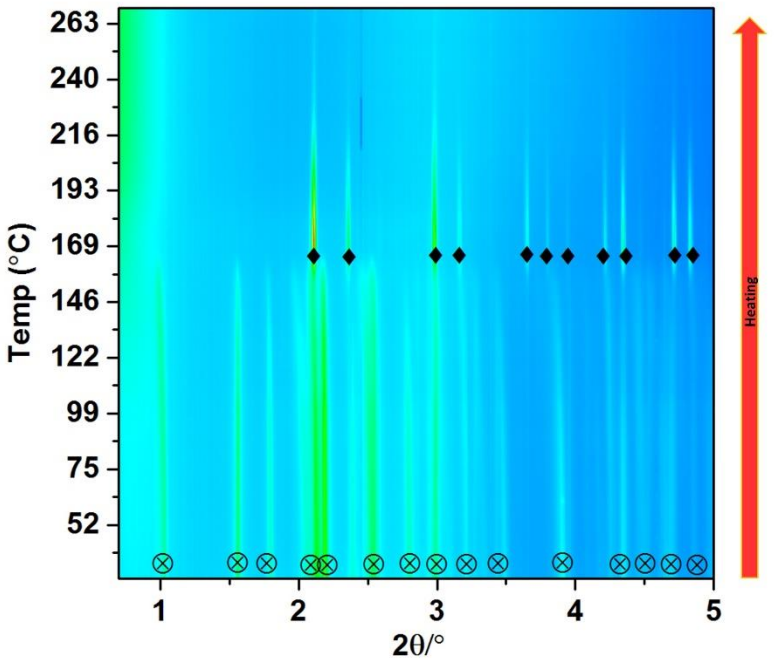

Figure S3 *In-situ* SR-XRPD data of $Nd(BH_4)_3S(CH_3)_2$ (**s4**) under p(Ar) = 1 bar. $\Delta T/\Delta t$ = 5 °C/min (λ = 0.2072 Å). Symbols: ⊗ for $Nd(BH_4)_3S(CH_3)_2$ and ♦ for α-$Nd(BH_4)_3$ ($Pa\bar{3}$).

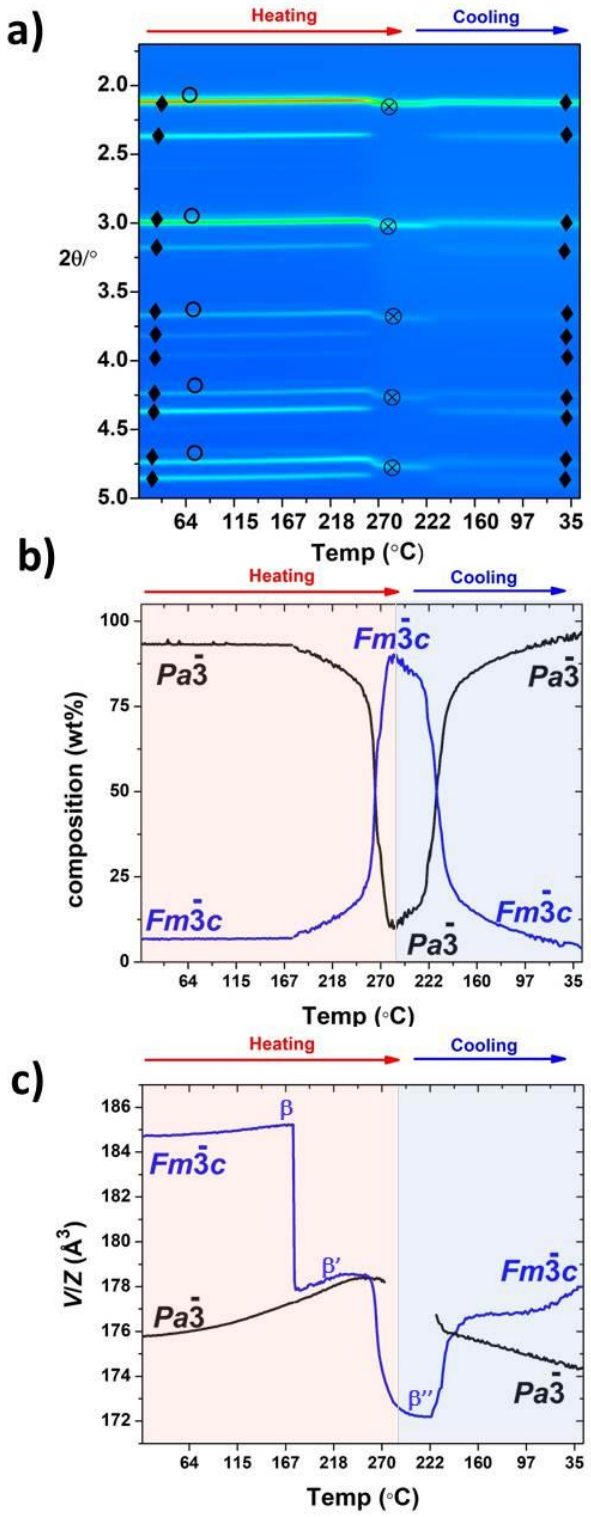

Figure S4 a) *In-situ* SR-XRPD data of $Nd(BH_4)_3$ (**s5**) under $p(H_2)$ = 98 bar. $\Delta T/\Delta t$ = 5 °C/min (λ = 0.2072 Å). b) Sample composition and c) *V*/*Z* of each phase extracted by Rietveld refinement of SR- XRPD data, c) symbols: ♦ for α-$Nd(BH_4)_3$ ($Pa\bar{3}$); ○ for β-$Nd(BH_4)_3$ ($Fm\bar{3}c$) and ⊗ for β''-$Nd(BH_4)_3$ ($Fm\bar{3}c$).

Table S1 Structural data extracted from Rietveld refinement of the SR-XRPD data for α, β, β' and β''-$Nd(BH_4)_3$ measured under $p(H_2)$ = 98 bar .

Sample	**α-$Nd(BH_4)_3$**	**β-$Nd(BH_4)_3$**	**β'-$Nd(BH_4)_3$**	**β''-$Nd(BH_4)_3$**
Crystal system	cubic	cubic	cubic	cubic
Space group	$Pa\bar{3}$	$Fm\bar{3}c$	$Fm\bar{3}c$	$Fm\bar{3}c$
***T* (°C)**	RT	134	190	269
***a* (Å)**	11.2034(5)	11.394(3)	11.3034(2)	11.1386(1)
RE-B	2.8306(1)	2.8485(8)	2.8259(4)	2.7847(3)
Z	8	8	8	8
***V* (Å^3)**	1406.21(11)	1479.21(70)	1444.2(3)	1381.95(21)
***V/Z* (Å^3)**	175.77	184.90	180.5	172.7
ρ (g cm^{-3})	1.8146	1.6953	1.7364	1.8146
ρv (H_2) (kg H_2.m^{-3})	116.2783	108.6329	111.2663	116.2783
ρm (H_2) (wt%)	6.4074	6.4074	6.4074	6.4074
Wt%	93(1)	7.9(0.6)	20.8(9)	100

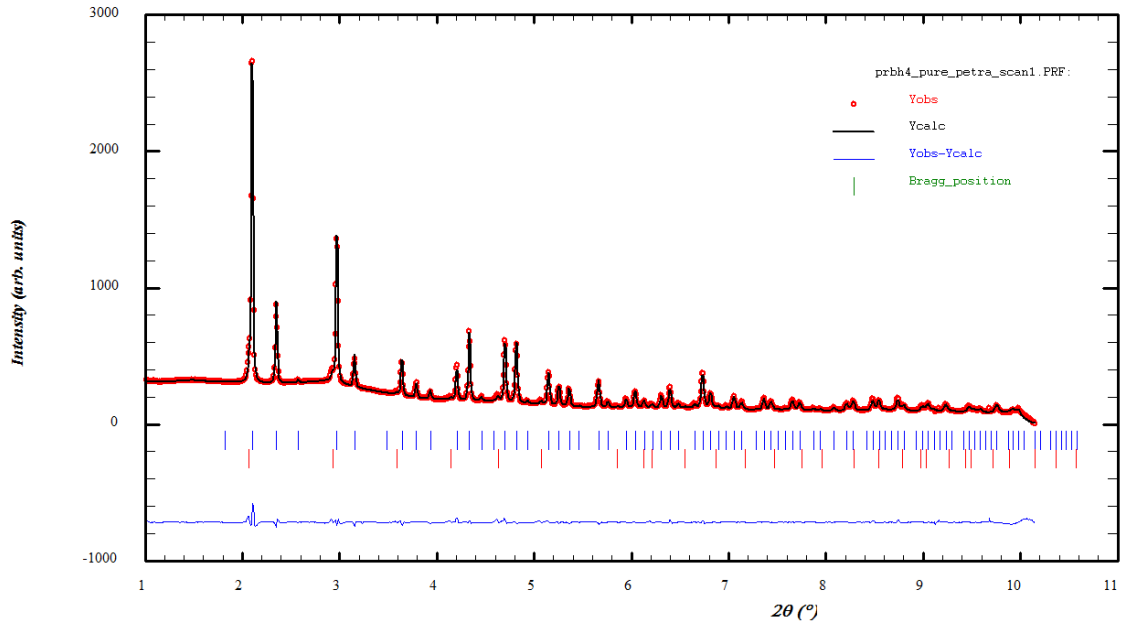

Figure S5 XRPD pattern and refinement of $Pr(BH_4)_3$ (**s3,** λ = 0.2072 Å). Red line: experimental data; black line: calculated pattern, blue line: difference pattern. Top blue tick for $Pa\bar{3}$ and bottom red ticks for $Fm\bar{3}c$ phases of $Pr(BH_4)_3$. R_{wp} = 4.99% (not corrected for background), χ^2 = 2810**.**

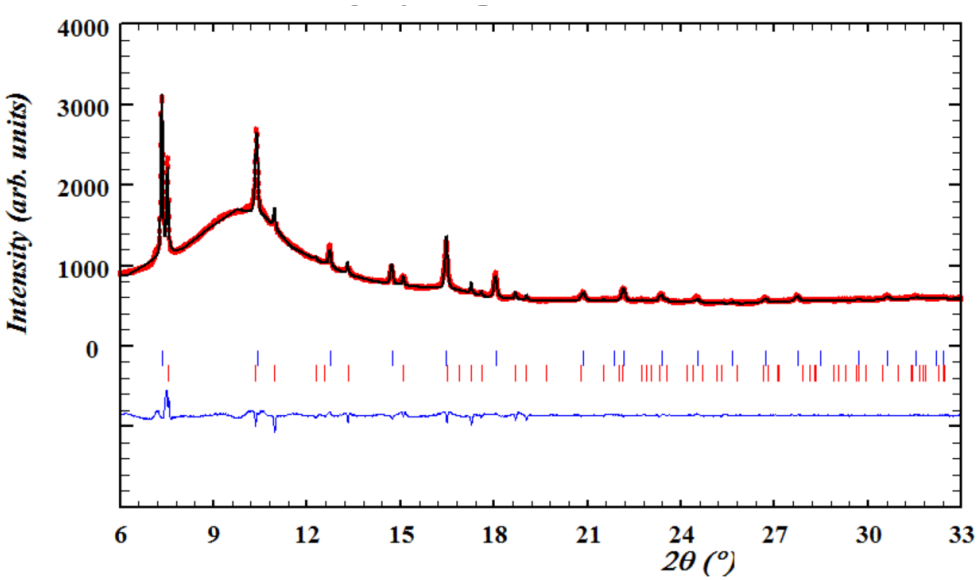

Figure S6 XRPD pattern and refinement of $Pr(BH_4)_3$ (**s3**, λ = 0.7129 Å) recorded at T = 176 °C and $p(H_2)$ = 40 bar. Red line: experimental data; black line: calculated pattern, blue line: difference pattern. Top blue ticks for $Fm\bar{3}c$ and bottom red ticks for $R\bar{3}c$ phases of $Pr(BH_4)_3$. R_{wp} = 2.22% (not corrected for background), χ^2 = 301.

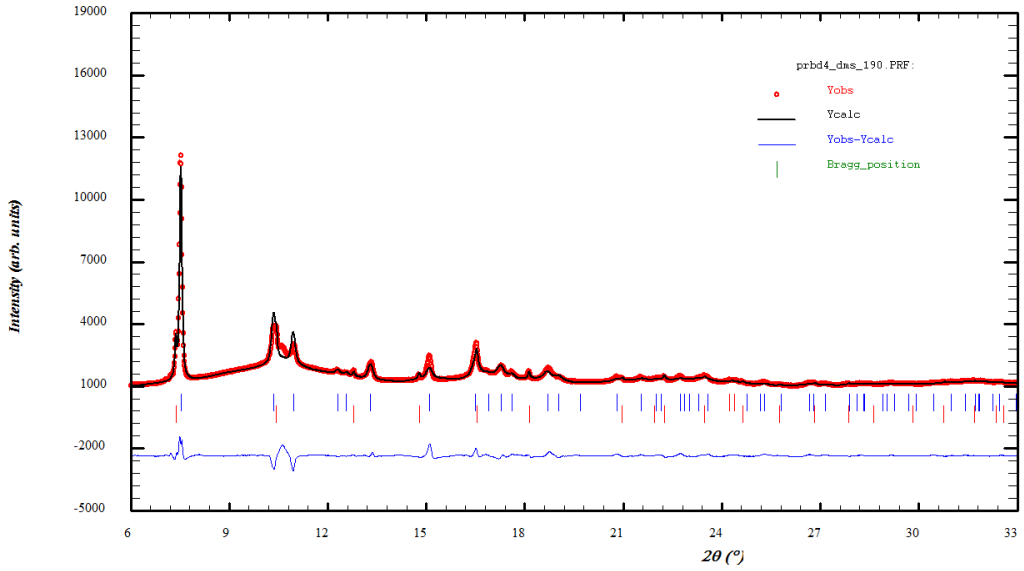

Figure S7 XRPD pattern and refinement of $Pr(^{11}BD_4)_3$ (**s1**, λ = 0.7129 Å) recorded at T = 190 °C and p(Ar) = 1 bar. Red line: experimental data; black line: calculated pattern, blue line: difference pattern. Top blue ticks $R\bar{3}c$ and bottom red ticks for $Fm\bar{3}c$ phase of $Pr(BH_4)_3$. R_{wp} = 4.66% (not corrected for background), χ^2 = 2450.

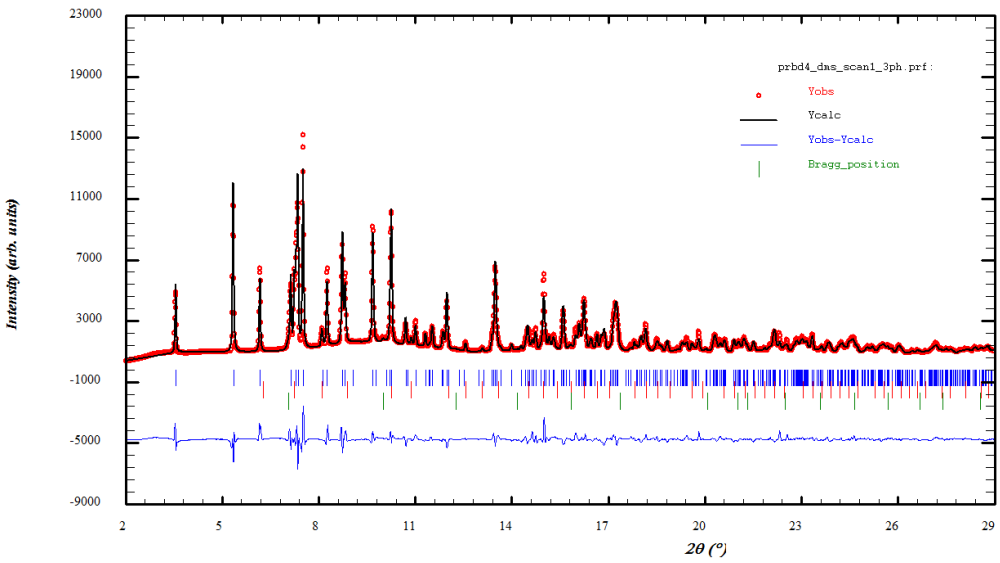

Figure S8 XRPD pattern and refinement of Pr($^{11}BD_4$)$_3$S(CH$_3$)$_2$ (**s1**, λ = 0.7129 Å) recorded at RT and *p*(Ar) = 1 bar. Red line: experimental data; black line: calculated pattern, blue line: difference pattern. Sample composition: 1. Top, blue ticks for Pr($^{11}BD_4$)$_3$S(CH$_3$)$_2$, middle red ticks: $Pa\bar{3}$ and bottom green ticks for $Fm\bar{3}c$ phase of Pr(BH$_4$)$_3$. R$_{wp}$ = 6.43 % (not corrected for background), χ^2 = 4770.

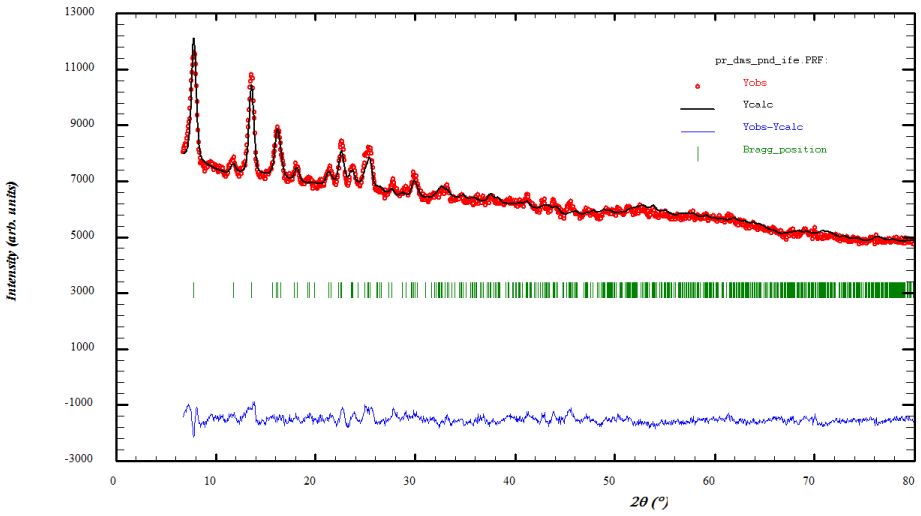

Figure S9 PND pattern and refinement of Pr($^{11}BD_4$)$_3$S(CH$_3$)$_2$ (λ = 1.5583 Å) recorded at RT. Red line: experimental data; black line: calculated pattern, blue line: difference pattern. Sample composition: R$_{wp}$ = 2.00 % (not corrected for background), χ^2 = 2.18. (This sample is obtained from another batch and therefore the sample composition does not match with sample s1)**.**

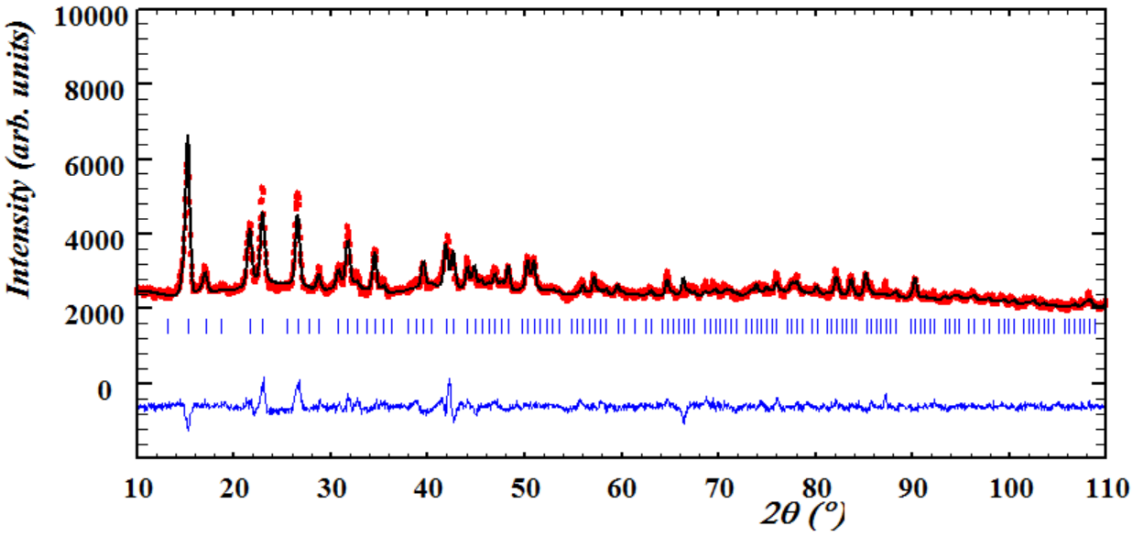

Figure S10 PND pattern and refinement of α-Pr($^{11}BD_4$)$_3$ (**s2**, λ = 1.494 Å) recorded at RT. Red line: experimental data; black line: calculated pattern, blue line: difference pattern. R_{wp} = 3.64 % (not corrected for background), χ^2 = 3.43**.**

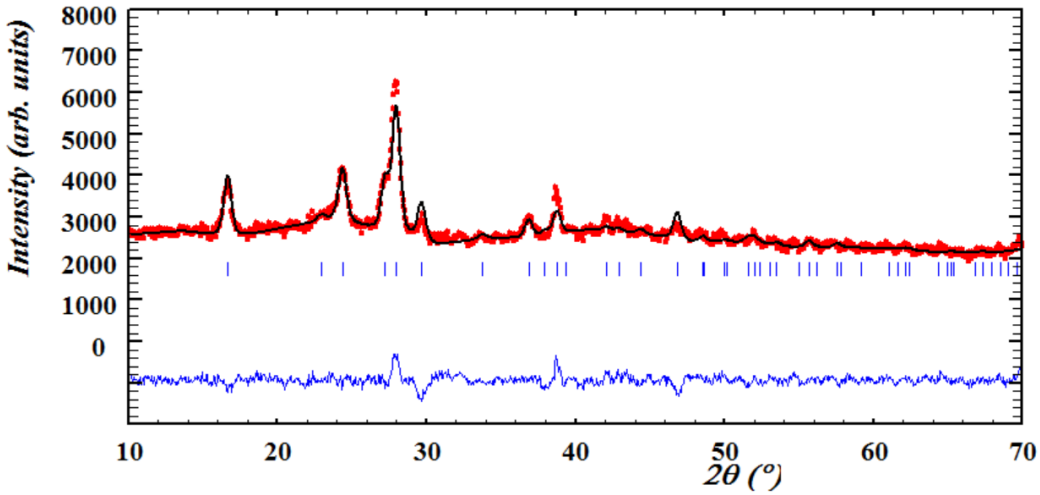

Figure S11 PND pattern and refinement of *r*-Pr($^{11}BD_4$)$_3$ (**s2**, λ = 1.5583 Å) recorded at 160 °C after heating to 200 °C for 30 min to induce the phase transition. Red line: experimental data; black line: calculated pattern, blue line: difference pattern. R_{wp} = 3.95 % (not corrected for background), χ^2 = 4.12**.**

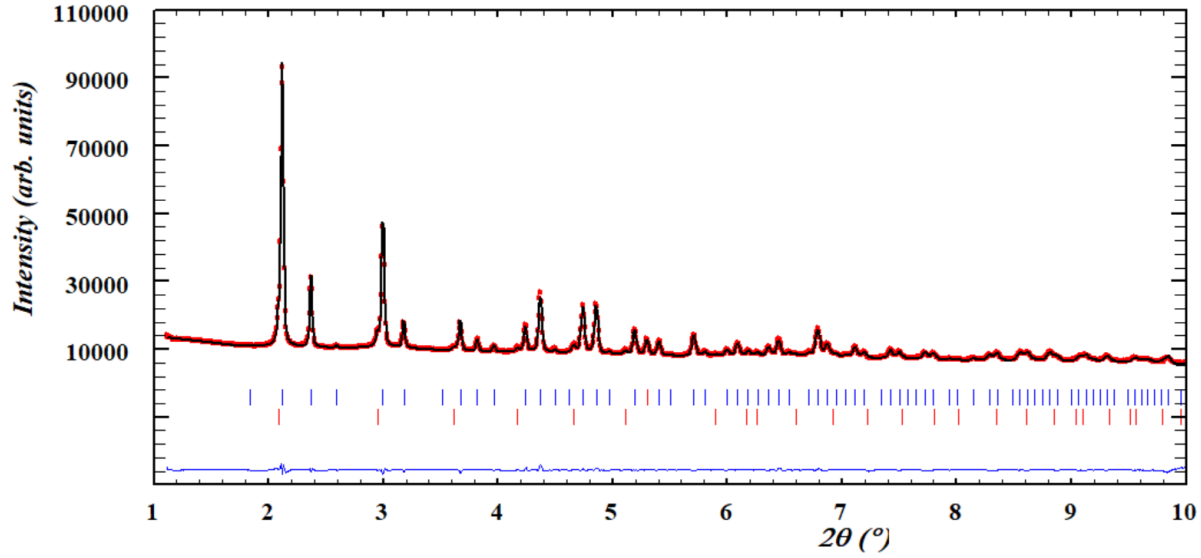

Figure S12 XRPD pattern and refinement of α-$Nd(BH_4)_3$ (**s5**, λ = 0.2072 Å) recorded at RT and $p(H_2)$ = 98 bar. Red line: experimental data; black line: calculated pattern, blue line: difference pattern. Sample composition: 1. Top, blue ticks for α-$Nd(BH_4)_3$ ($Pa\bar{3}$) and bottom red ticks for β-$Pr(BH_4)_3$ ($Fm\bar{3}c$). R_{wp} = 2.38% (not corrected for background), χ^2 = 1490.

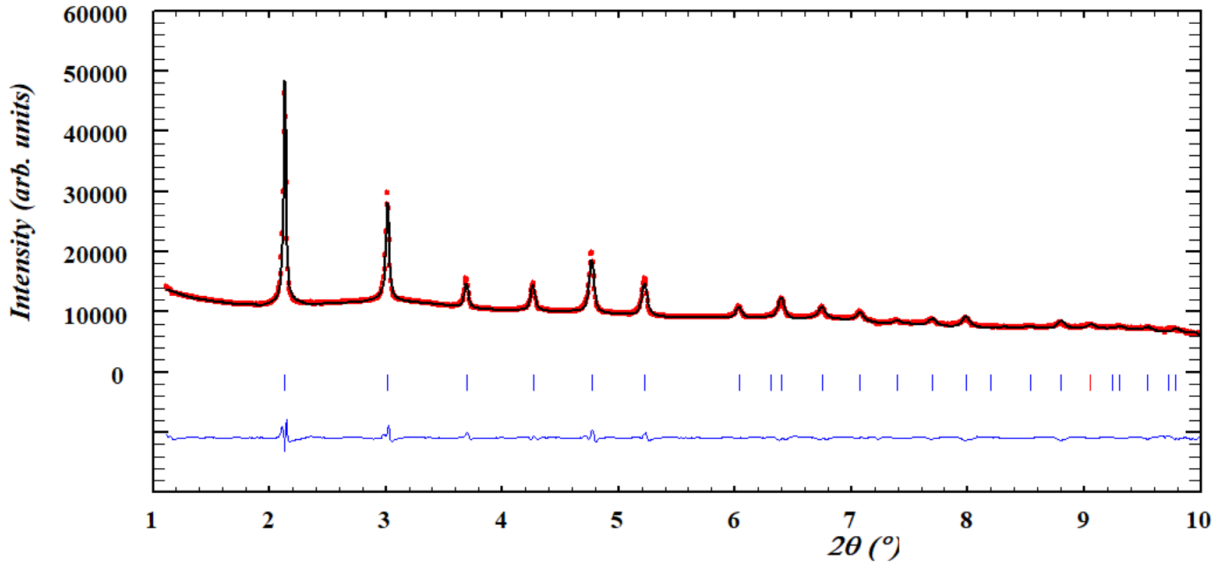

Figure S13 XRPD pattern and refinement of β-$Nd(BH_4)_3$ (**s5**, λ = 0.2072 Å) recorded at 269 °C and $p(H_2)$ = 98 bar. Red line: experimental data; black line: calculated pattern, blue line: difference pattern. Blue ticks for β-$Pr(BH_4)_3$($Fm\bar{3}c$). R_{wp} = 4.59% (not corrected for background), χ^2 = 5970.

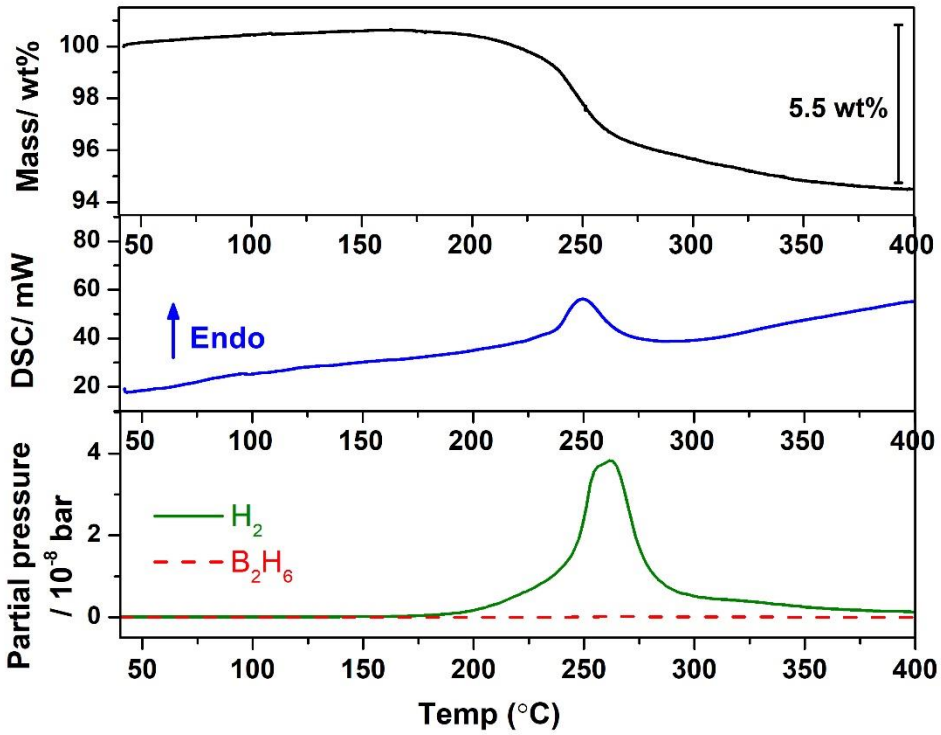

Figure S14 TGA-DSC-MS data for $Nd(BH_4)_3$ (**s4**) heated from RT to 400 °C. Upper part: The TGA curve in black, Middle, DSC curve in blue and the corresponding MS signals in lower part for hydrogen and diborane presented by green and red curves, respectively. ($\Delta T/\Delta t$ = 5 °C/min).

Table S2 Structural data of different polymorphs of $Pr(^{11}BD_4)_3$ extracted from Rietveld refinements of the XRPD data of $Pr(^{11}BD_4)_3S(CH_3)_2$ (**s1**) measured in p(Ar) = 1 bar, Figure 3.

sample	**β-Pr($^{11}BD_4$)$_3$**	**β'-Pr($^{11}BD_4$)$_3$**	**β''-Pr($^{11}BD_4$)$_3$**	**r-Pr($^{11}BD_4$)$_3$**
Crystal system	cubic	Cubic	cubic	trigonal
Space group	$Fm\bar{3}c$	$Fm\bar{3}c$	$Fm\bar{3}c$	$R\bar{3}c$
***T* (°C)**	174	185	190	190
***a* (Å)**	11.4535(17)	11.3003(6)	11.0983(10)	7.4989(10)
***b* (Å)**	-	-	-	
***c* (Å)**	-	-	-	19.904(6)
***β* (°)**				120
RE-B (Å)	2.8634(4)	2.8251(2)	2.7746(3)	2.9236(4)
Z	8	8	8	6
***V* (Å^3)**	1502.50(39)	1443.01(13)	1367.01(21)	969.32(34)
***V*/*Z* (Å^3)**	187.81	180.37	170.88	161.55
Wt%	4.5(0.3)	20.5(0.5)	12.2(0.3)	87.8(0.9)

Table S3 Structural data of different polymorphs of $Pr(BH_4)_3$ extracted from Rietveld refinements of the XRPD data of $Pr(BH_4)_3$ (**s3**) measured in $p(H_2)$ = 40 bar, Figure 4.

sample	**β-Pr(BH_4)$_3$**	**β'-Pr(BH_4)$_3$**	**β''-Pr(BH_4)$_3$**	***r*-Pr(BH_4)$_3$**
Crystal system	cubic	cubic	Cubic	trigonal
Space group	$Fm\bar{3}c$	$Fm\bar{3}c$	$Fm\bar{3}c$	$R\bar{3}c$
***T* (°C)**	170	185	190	190
***a* (Å)**	11.458(2)	11.3283(6)	11.1438(7)	7.4831(12)
***c* (Å)**	-	-	-	19.995(5)
***β* (°)**	-	-	-	120
RE-B (Å)	2.8645(5)	2.8321(2)	2.7859(2)	2.9237(3)
Z	8	8	8	6
***V* (Å^3)**	1504.27(45)	1453.77(13)	1383.88(15)	969.65(30)
***V*/*Z* (Å^3)**	188.03	181.72	172.98	161.61
Wt%	5.6(0.3)	22.92(0.3)	63.6(0.7)	36.3(0.6)